

PAPER

Parameter Estimation of Fractional Bandlimited LFM Signals Based on Orthogonal Matching Pursuit

Xiaomin LI^{†,††a)}, *Nonmember*, Huali WANG^{†††b)}, *Member*, and Zhangkai LUO^{††††c)}, *Student Member*

SUMMARY Parameter estimation theorems for LFM signals have been developed due to the advantages of fractional Fourier transform (FrFT). The traditional estimation methods in the fractional Fourier domain (FrFD) are almost based on two-dimensional search which have the contradiction between estimation performance and complexity. In order to solve this problem, we introduce the orthogonal matching pursuit (OMP) into the FrFD, propose a modified optimization method to estimate initial frequency and final frequency of fractional bandlimited LFM signals. In this algorithm, the differentiation fractional spectrum which is used to form observation matrix in OMP is derived from the spectrum analytical formulations of the LFM signal, and then, based on that the LFM signal has approximate rectangular spectrum in the FrFD and the correlation between the LFM signal and observation matrix yields a maximal value at the edge of the spectrum (see Sect. 3.3 for details), the edge spectrum information can be extracted by OMP. Finally, the estimations of initial frequency and final frequency are obtained through multiplying the edge information by the sampling frequency resolution. The proposed method avoids reconstruction and the traditional peak-searching procedure, and the iterations are needed only twice. Thus, the computational complexity is much lower than that of the existing methods. Meanwhile, since the vectors at the initial frequency and final frequency points both have larger modulus, so that the estimations are closer to the actual values, better normalized root mean squared error (NRMSE) performance can be achieved. Both theoretical analysis and simulation results demonstrate that the proposed algorithm bears a relatively low complexity and its estimation precision is higher than search-based and reconstruction-based algorithms.

key words: linear frequency modulation signal, parameter estimation, orthogonal matching pursuit, fractional Fourier transform

1. Introduction

Fractional Fourier transform (FrFT) is a powerful tool for analyzing LFM signals which are also known as chirp signals [1]. FrFT uses a transform kernel which essentially allows the signal in the time-frequency domain to be projected onto a line of arbitrary angle. The definition of FrFT is denoted by [2]:

Manuscript received May 15, 2019.

[†]The author is with School of Electronic and Optical Engineering, Nanjing University of Science and Technology, Nanjing 210094, China.

^{††}The author is with School of Mechanical and Electrical Engineering, Henan Institute of Science and Technology, Xinxiang 453003, China.

^{†††}The author is with College of Communication Engineering, The Army Engineering University of PLA, Nanjing 210007, China.

^{††††}The author is with Science and Technology on Complex Electronic System Simulation Laboratory, Space Engineering University, Beijing 101416, China.

a) E-mail: 213104000049@njjust.edu.cn

b) E-mail: huali.wang@ieee.org (Corresponding author)

c) E-mail: luo.zhangkai@126.com

DOI: 10.1587/transfun.E102.A.1448

$$X_p(u) = \{F_p[x(t)]\}(u) = \int_{-\infty}^{\infty} x(t) K_p(t, u) dt \quad (1)$$

Where F_p denotes the FrFT operator. The kernel function is denoted by:

$$K_p(t, u) = \begin{cases} A_\alpha \exp j\pi \left[(t^2 + u^2) \cot \alpha - 2ut \csc \alpha \right], & \alpha \neq n\pi \\ \delta(t - u), & \alpha = n\pi \\ \delta(t + u), & \alpha = (2n + 1)\pi \end{cases} \quad (2)$$

Where $A_\alpha = \sqrt{1 - j \cot \alpha}$, and $\alpha = \frac{p\pi}{2}$ is the transform angle. FrFT can be interpreted as a signal decomposition in terms of a chirp basis as its kernel is constituted by chirp functions, so FrFT has a notable potential for analyzing chirp signals [1], [3]. For the LFM signal detection and parameter estimation, FrFT is densely used by making use of the change of the concentration, or equivalently the support. In the fractional Fourier domain (FrFD), support of LFM signals change associated with the transform angle and there exists an optimum transform angle in which the energy of chirp signals are most concentrated [4], [5]. when an LFM signal is transformed by FrFT at its optimum angle, transform kernel acts as a matched filter. Therefore, an optimum LFM detection and estimation can be done by sweeping all of the angles and finding the correct angle that maximizes the absolute amplitude. Almost all successful methods employing FrFT use the maximum peak of sweep in the FrFD [4], [6]–[11], which is an easy method to realize. And obviously, the search-based algorithms above require numerous extra calculations and have the contradiction between estimation performance and complexity.

In recent years, numerous researchers have explored the parameter estimation problem of chirp signals from different aspects [1], [9], [12]–[22]. Inspired by the recently-developed sparse reconstruction method [23]–[28], we propose a fast and high accuracy parameter estimation method for LFM signals in the FrFD based on orthogonal matching pursuit (OMP). In this algorithm, We construct the observation matrix through the differentiation spectrum, and prove that the LFM signal and observation matrix are most relevant at the edge of the fractional spectrum, so the fractional spectrum edge information can be extracted by OMP. And the estimations of initial frequency and final frequency can be gotten through multiplying the sampling frequency resolution by the edge information.

Neither reconstruction nor peak-searching are needed in the proposed method, which can reduce the computa-

tional complexity greatly. And the estimation precision is higher than existing algorithms because of the larger modulus the vectors at the initial frequency and final frequency points have (see Sect. 3.3 for details). Simulation results demonstrate that the proposed algorithm has better normalized root mean squared error (NRMSE) performance.

The remainder of this paper is organized as follows: In Sect. 2, the basic preliminaries is presented. The new algorithm is proposed in Sect. 3. In Sect. 4, the parameters estimation performance is simulated and analyzed. Section 5 is the conclusion.

2. Preliminaries

2.1 Simplified Fractional Fourier Transform (SFrFT)

FrFT is an extension of the ordinary Fourier transform (FT), which essentially allows the signal in the time-frequency domain to be projected onto a line of arbitrary angle [29]. Simplified fractional Fourier transform (SFrFT) [30] has the same effect as FrFT of order α for filter design, but it is simpler to implement digitally than the original FrFT. And the first type of α -th-order SFRFT is defined as [30]:

$$\bar{Y}_\alpha(u) = (j2\pi)^{-\frac{1}{2}} \times \int_{-\infty}^{\infty} \exp(-jut + jt^2 \cot \alpha/2) y(t) dt \quad (3)$$

where α is the SFrFT order. The inverse SFrFT is denoted as follows:

$$y(t) = (j/2\pi)^{\frac{1}{2}} \exp(-ju^2 \cot \alpha/2) \times \int_{-\infty}^{\infty} \exp(jut) \bar{Y}_\alpha(u) dt \quad (4)$$

The digital implementation of SFrFT (DSFrFT) is given by [30]

$$F_\alpha[m] = (j2\pi)^{-\frac{1}{2}} \Delta t \sum_{n=-N}^N \exp\left(-j \frac{2\pi mn}{2N+1} + \frac{j}{2} n^2 \cot \alpha (\Delta t)^2\right) \cdot y[n] \quad (5)$$

Where $y[n] = y[n\Delta t]$, $F_\alpha[m] = F_\alpha[m\Delta u]$, $m, n = -N, -N+1, N$, Δt and Δu are the sample spacing in temporal domain and simplified fractional Fourier domain (SFrFD) respectively. And $\Delta t \Delta u = 2\pi / (2N+1)$. We can also write (5) in matrix form, expressed as

$$F_\alpha = c_1 O_F^\alpha y$$

Where $c_1 = (j2\pi)^{-\frac{1}{2}} \Delta t$, $(O_F^\alpha)^{-1} = (O_F^\alpha)^*$, $*$ denotes the transposed conjugate operator, and O_F^α is a $(2N+1) \times (2N+1)$ unitary matrix whose element $[O_F^\alpha]_{mn}$ at the m row, n column has the following form:

$$[O_F^\alpha]_{mn} = \exp\left[-j \frac{2\pi(m-N-1)(n-N-1)}{2N+1}\right] \cdot \exp\left[j(n-N-1)^2 \cot \alpha (\Delta t)^2 / 2\right]$$

where $[\cdot]$ returns the nearest integer towards positive infinity. With the change of α , the frequency axis of the SFrFT is located in different positions, and more abundant information about the frequency characteristics of the signal can be obtained compared to the FT.

2.2 Fractional Bandlimited LFM Signal and Its Spectral Features in SFrFD

A fractional bandlimited LFM signal $f(t)$ has finite energy. The SFrFT of $f(t)$ is zero outside the region $(-u_0 - u_\alpha, -u_0 + u_\alpha) \cup (u_0 - u_\alpha, u_0 + u_\alpha)$.

i.e.

$$F_\alpha(u) = \begin{cases} F_\alpha(u), & u_0 - u_\alpha \leq |u| \leq u_0 + u_\alpha \\ 0, & \text{otherwise} \end{cases} \quad (6)$$

Where $2u_\alpha$ is the fractional bandwidth of $f(t)$. According to Parseval's theorem, the bandlimited LFM signal can also be expressed as:

$$\int_{-\infty}^{\infty} |f(t)|^2 dt = \int_{-u_h}^{-u_l} |F_\alpha(u)|^2 du + \int_{u_l}^{u_h} |F_\alpha(u)|^2 du$$

where $u_h = u_0 + u_\alpha$, and $u_l = u_0 - u_\alpha$.

The LFM signal model is given by

$$x(t) = A \cdot \exp(j2\pi f_0 t + j\pi K_{lfm} t^2) \quad (7)$$

Where f_0 is the initial frequency, A is the amplitude of $x(t)$ which could be random or fixed. K_{lfm} is the modulation rate.

And using the results in Appendix, for the LFM signal whose duration time is $[-\frac{T_d}{2}, \frac{T_d}{2}]$, when $(K_{lfm} + \cot \alpha / 2\pi) T_d^2 \gg 1$, its amplitude spectrum in SFrFD is

$$|X_\alpha(u)| \approx \frac{1}{\sqrt{K_{lfm} + \cot \alpha / 2\pi}} \cdot \text{rect}\left(\frac{u - 2\pi u_0 \csc \alpha}{B'}\right) \quad (8)$$

and its phase spectrum in SFrFD is

$$\theta(u) \approx -\frac{\pi(u - 2\pi u_0 \csc \alpha)^2}{K_{lfm} + \cot \alpha / 2\pi} + \frac{\pi}{4} \quad (9)$$

Where B' is the width of the spectrum in SFrFD, $K'_{lfm} = K_{lfm} + \cot \alpha / 2\pi$, and α is the fractional orders. And according to (6) and (8), the LFM signal $x(t)$ whose duration time is $[-\frac{T_d}{2}, \frac{T_d}{2}]$ is a fractional bandlimited signal.

3. Proposed Parameter Estimation Method for Fractional Bandlimited LFM Signals

3.1 Method Description

In this part, we propose an optimization method to estimate initial frequency and final frequency of fractional bandlimited LFM signals by introducing the OMP. The proposed method is based on two principles. First, the LFM signal has a rectangular spectrum in the SFrFD of α -th order when

$T_d \cdot \sqrt{|K_{lfm} + \cot \alpha|} \gg 1$ (see Appendix for details), and the correlation between the LFM signal and observation matrix yields a maximal value at the edge of the fractional spectrum (see Sect. 3.3 for details). Second, OMP algorithm have the ability to search the maximum correlation information.

In the proposed method, the differentiation spectrum which is used to form the observation matrix is derived from the spectrum analytical formulations of the LFM signal in the FrFD, and then the correlation between the LFM signal and observation matrix is proved to be the largest at the edge of the fractional spectrum, as a result, the spectrum edge information can be extracted by OMP. Finally, multiply the sampling frequency resolution by the edge information to get the estimations of initial frequency and final frequency.

There are only two iterations in the method, neither reconstruction nor the traditional peak-searching procedures are needed, thus, the computational complexity is much lower than the existing methods. Meanwhile, since the vectors at the initial frequency and final frequency points both have larger amplitude, so that better NRMSE performance can be achieved as well.

3.2 The Differential Procedure for the Fractional Spectrum of the LFM Signal

The fractional bandlimited LFM signals can be depicted as

$$\begin{aligned}
 y_m &= A \cdot e^{j[2\pi(n_i n / K + K_{lfm} n^2 / 2K^2)]}_{n=0,1,\dots,K-1} \\
 &= A \cdot e^{j\left\{2\pi\left[\frac{n_i}{K}\left(n - \frac{n^2}{2K}\right) + \frac{n_h}{K} \frac{n^2}{2K}\right]\right\}}_{n=0,1,\dots,K-1} \quad (10) \\
 &= [y_m(0) \quad y_m(1) \quad \dots \quad y_m(K-1)]^T
 \end{aligned}$$

where n_i is the initial frequency point, n_h is the final frequency point. K_{lfm} is the modulation rate. K is the number of sampling data.

The DSFrFT of y_m is [30]

$$F_\alpha = c_1 O_F^\alpha y_m$$

the differentiating process for F_α can be expressed as

$$y = \Gamma' \cdot F_\alpha = \Gamma' \cdot c_1 O_F^\alpha y_m \quad (11)$$

where $\Gamma' = \begin{bmatrix} 1 & -1 & \dots & 0 \\ 0 & 1 & \ddots & 0 \\ 0 & \ddots & \ddots & -1 \\ 0 & \dots & 0 & 1 \end{bmatrix}_{K \times K}$

is the differentiating matrix. $c_1 = (j2\pi)^{-1/2} \Delta t$,

$$O_F^\alpha = \begin{bmatrix} O_F^\alpha(1,1) & O_F^\alpha(1,2) & \dots & O_F^\alpha(1,K) \\ O_F^\alpha(2,1) & O_F^\alpha(2,2) & \dots & O_F^\alpha(2,K) \\ \vdots & \vdots & \ddots & \vdots \\ O_F^\alpha(K,1) & O_F^\alpha(K,2) & \dots & O_F^\alpha(K,K) \end{bmatrix}_{K \times K}$$

is the DSFrFT matrix, and O_F^α is unitary matrix. The elements of matrix O_F^α are:

$$O_F^\alpha(m, n) = \exp\left[-j \frac{2\pi(m-N'-1)(n-N'-1)}{2N'+1}\right]$$

$$\begin{aligned}
 &\cdot \exp\left[j(n - N' - 1)^2 \cot \alpha (\Delta t)^2 / 2\right] \\
 m, n &= 1, \dots, N', \dots, K, N' = \left\lceil \frac{K-1}{2} \right\rceil, \Delta t = \frac{1}{f_s}
 \end{aligned}$$

From Eq. (11),

$$y_m = (\Gamma' \cdot c_1 O_F^\alpha)^{-1} \cdot y = G' \cdot y \quad (12)$$

Where

$$\begin{aligned}
 G' &= (\Gamma' \cdot c_1 O_F^\alpha)^{-1} = (j/2\pi)^{1/2} / (K\Delta t) \cdot \\
 &\begin{bmatrix} \sum_{n=1}^1 O_F^\alpha(1,n) & \sum_{n=1}^2 O_F^\alpha(1,n) & \dots & \sum_{n=1}^k O_F^\alpha(1,n) \\ \sum_{n=1}^1 O_F^\alpha(2,n) & \sum_{n=1}^2 O_F^\alpha(2,n) & \dots & \sum_{n=1}^k O_F^\alpha(2,n) \\ \vdots & \vdots & \ddots & \vdots \\ \sum_{n=1}^1 O_F^\alpha(K,n) & \sum_{n=1}^2 O_F^\alpha(K,n) & \dots & \sum_{n=1}^k O_F^\alpha(K,n) \end{bmatrix}_{K \times K}^*
 \end{aligned}$$

3.3 The Correlation between G' and y_m

Assume the initial residual $res_0 = y_m$, observation matrix $G' = (\Gamma' \cdot c_1 O_F^\alpha)^{-1}$, so the correlation between res_0 and G' can be computed according to their inner product as follows:

$$\begin{aligned}
 |\langle res_0, G' \rangle| &= (j/2\pi)^{1/2} / (K\Delta t) \cdot \\
 &\begin{bmatrix} \left| \sum_{n=1}^1 O_F^\alpha(n,1) y_m(1) + \dots + \sum_{n=1}^1 O_F^\alpha(n,k) y_m(k) \right| \\ \left| \sum_{n=1}^2 O_F^\alpha(n,1) y_m(1) + \dots + \sum_{n=1}^2 O_F^\alpha(n,k) y_m(k) \right| \\ \vdots \\ \left| \sum_{n=1}^K O_F^\alpha(n,1) y_m(1) + \dots + \sum_{n=1}^K O_F^\alpha(n,k) y_m(k) \right| \end{bmatrix}_{K \times 1} \quad (13)
 \end{aligned}$$

Where $\langle \cdot \rangle$ denotes the inner product operator. Since the DSFrFT of $y_m(n)$ is

$$F_\alpha(m) = c_1 \sum_{n=1}^K O_F^\alpha(m,n) \cdot y_m(n)$$

Equation (13) can be reduced to:

$$\begin{aligned}
 |\langle res_0, G' \rangle| &= [|\langle res_0, g'_1 \rangle| |\langle res_0, g'_2 \rangle| \dots |\langle res_0, g'_K \rangle|]^T \\
 &= (j/2\pi)^{1/2} / (K\Delta t) \cdot \\
 &\begin{bmatrix} |F_\alpha(1)| \\ |F_\alpha(1) + F_\alpha(2)| \\ \vdots \\ |F_\alpha(1) + F_\alpha(2) + \dots + F_\alpha(k-1)| \\ |F_\alpha(1) + F_\alpha(2) + \dots + F_\alpha(k-1) + F_\alpha(k)| \end{bmatrix}_{K \times 1} \\
 &= (j/2\pi)^{1/2} / (K\Delta t) \cdot
 \end{aligned}$$

$$\begin{bmatrix} \left| \sum_{m=1}^1 F_\alpha(m) \right| \left\| \sum_{m=1}^2 F_\alpha(m) \right\| \dots \left\| \sum_{m=1}^K F_\alpha(m) \right\| \end{bmatrix}^T \quad (14)$$

According to (14), $|\langle res_0, g'_k \rangle|$, the k th element of $|\langle res_0, G' \rangle|$, denotes the summation of the first k terms from $F_\alpha(m)$, which is the DSFrFT of $y_m(n)$. And for the LFM signal y_m , when $T_d \cdot \sqrt{|K_{lfm} + \cot \alpha|} \gg 1$, its amplitude spectrum and phase spectrum in α -th order discrete time simplified fractional Fourier domain (DTSFrFD) are respectively:

$$|X_\alpha(u)| \approx \frac{A}{\sqrt{|K_{lfm} + \cot \alpha|}} \cdot \text{rect}\left(\frac{u - 2\pi u_0 \csc \alpha}{B'}\right) \quad (15)$$

$$\theta(u) \approx \frac{\pi(u - 2\pi u_0 \csc \alpha)^2}{|K_{lfm} + \cot \alpha|} + \frac{\pi}{4} \quad (16)$$

Substitute (15) and (16) into (14),

$$|\langle res_0, g'_k \rangle| = \begin{cases} 0, & k < n_l \\ \frac{(j/2\pi)^{\frac{1}{2}}}{K\Delta t} \cdot \frac{A}{\sqrt{|K_{lfm} + \cot \alpha|}} \cdot \sum_{m=1}^{k-n_l} e^{j\phi(m)}, & n_l \leq k \leq n_h \\ \frac{(j/2\pi)^{\frac{1}{2}}}{K\Delta t} \cdot \frac{A}{\sqrt{|K_{lfm} + \cot \alpha|}} \cdot \sum_{m=1}^{k-n_l} e^{j\phi(m)}, & k > n_h \end{cases} \quad (17)$$

Where $\phi(m) = -\frac{\pi(m\Delta)^2}{|K_{lfm} + \cot \alpha|} + \frac{\pi}{4}$, $0 \leq m \leq n_h - n_l$, and

$$\Delta\phi(m) = \phi(m) - \phi(m+1) = \pi \frac{(2m+1)\Delta^2}{|K_{lfm} + \cot \alpha|} \quad (18)$$

when $n_l \leq k \leq n_h$, $|\langle res_0, g'_k \rangle|$ can be expressed as the sum of $\frac{(j/2\pi)^{\frac{1}{2}}}{K\Delta t} \cdot \frac{A}{\sqrt{|K_{lfm} + \cot \alpha|}} \cdot e^{j\phi(m)}$, whose phase changes nonlinearly in Eq. (18) as Fig. 1.

Let vector $B = \frac{(j/2\pi)^{\frac{1}{2}}}{K\Delta t} \cdot \frac{A}{\sqrt{|K_{lfm} + \cot \alpha|}} \cdot e^{j\phi(m)}$. And Fig. 1 also shows that vector B with constant magnitude, moves clockwise on a circle. Meanwhile, $\phi(m)$, the phase of B , increases with an interval of $\Delta\phi(m)$, therefore $|\langle res_0, g'_k \rangle|$ will increase at first and then decrease. According to (18), $\Delta\phi(m)$ increases as B moves along the circle clockwise, the

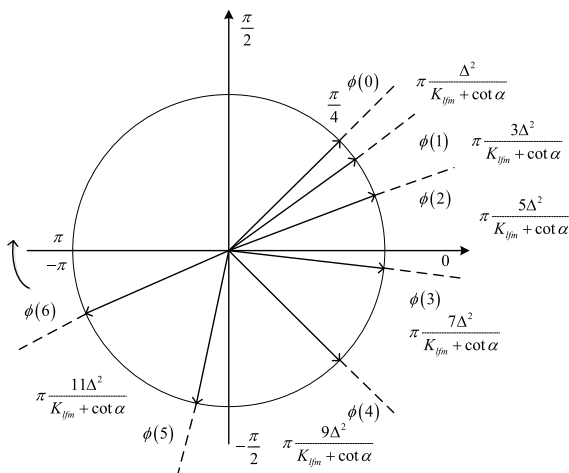


Fig. 1 The vector B with constant magnitude.

accumulated phase energy of $|\langle res_0, g'_k \rangle|$ reaches its maximum value within the first cycle. And this maximum value is corresponding to the estimation of initial frequency. Similarly, when differentiating matrix is

$$\Gamma = \begin{bmatrix} 1 & 0 & \cdots & 0 \\ -1 & 1 & \ddots & 0 \\ 0 & \ddots & \ddots & 0 \\ 0 & \cdots & -1 & 1 \end{bmatrix}_{K \times K},$$

observation matrix is $G = (\Gamma \cdot c_1 O_F^\alpha)^{-1}$,

$$|\langle res_0, G \rangle| = [|\langle res_0, g_1 \rangle| |\langle res_0, g_2 \rangle| \cdots |\langle res_0, g_K \rangle|]^T = (j/2\pi)^{1/2} / (K\Delta t) \cdot \begin{bmatrix} |F_\alpha(1) + F_\alpha(2) + F_\alpha(3) + \cdots + F_\alpha(K)| \\ |F_\alpha(2) + F_\alpha(3) + \cdots + F_\alpha(K)| \\ \vdots \\ |F_\alpha(K)| \end{bmatrix}_{K \times 1} \quad (19)$$

$$= (j/2\pi)^{1/2} / (K\Delta t) \cdot \left[\left| \sum_{m=1}^K F_\alpha(m) \right| \left| \sum_{m=2}^K F_\alpha(m) \right| \cdots \left| \sum_{m=K}^K F_\alpha(m) \right| \right]^T$$

And a similar analysis can be perform for $|\langle res_0, g_k \rangle|$, as a result, the maximum value of $|\langle res_0, g_k \rangle|$ is corresponding to the estimation of final frequency.

3.4 The Parameter Estimation Procedures Using OMP

Assume res_0 is the residual, i is the iteration count, Λ_0 is a set of indices of the nonzero channel coefficients. g'_k ($k = 1, 2, \dots, K$) is the columns of observation matrix G' . And $y_m = G' \cdot y$. Accordingly, the initial frequency estimation procedures of the proposed method is summarized in Algorithm 1.

Algorithm 1: the initial frequency estimation

- (1) Initialize $res_0 = y_m$, $i = 1$ and $\Lambda_0 = \emptyset$.
 - (2) Determine the new index λ'_i by selecting the maximum absolute value of the correlation between G' and previous residual res_0 . That is, $\lambda'_i = \arg \max_{k=1,2,\dots,N/2} |\langle res_{i-1}, g'_k \rangle|$.
 - (3) combine the newly selected index λ'_i with the index Λ_{i-1} , i.e., $\Lambda_i = \Lambda_{i-1} \cup \{\lambda'_i\}$. Compute the $y_i = \arg \min_y \|y_m - G'_{\Lambda_i} y\|_2$. Compute the new residual $res_i = y_m - G'_{\Lambda_i} y_i$.
 - (4) Set $i = i + 1$ if $i < 3$ go to step 2.
-

The stopping criterion in Algorithm 1 is $i = 3$, which means that two iterations for $y_m = G' \cdot y$ is required. As a result, λ'_1 and λ'_2 , the index which are corresponding to the maximum values of the correlation between G' and residual

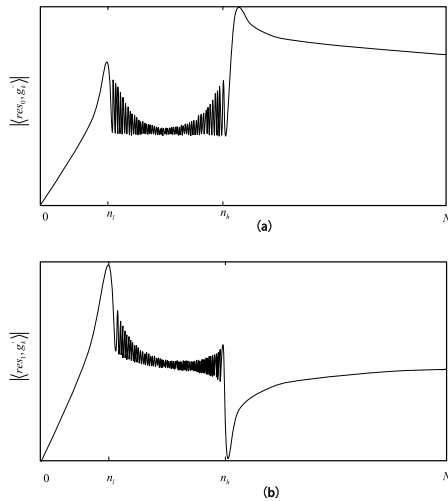


Fig. 2 The relationship between $|\langle res_{i-1}, g'_k \rangle|$ and the fractional “frequency”.

within each iterations, are obtained. And the estimated initial frequency of LFM signal in DTSFrFD is $\min(\lambda'_1, \lambda'_2) \Delta$, where $\Delta = 1/KT_s$, T_s is the sampling interval.

Similarly, when observation matrix is $G = (\Gamma \cdot c_1 O_F^\alpha)^{-1}$, conduct two iterations on $y_m = G \cdot y$ to generate two indexes λ_1, λ_2 . Then the estimated final frequency in DTSFrFD is $\max(\lambda_1, \lambda_2) \Delta$, where $\Delta = 1/KT_s$. Figure 2 illustrates the relationship between $|\langle res_{i-1}, g'_k \rangle|$, $i = 1, 2$ and the fractional “frequency”. Figure 2(a) shows that there are two maximum values at n_l and n_h respectively after the first iteration. Thus the index λ'_1 corresponds to either n_l or n_h . Compared with Fig. 2(a), $|\langle res_1, g'_k \rangle|$ has a smaller value at n_h as shown in Fig. 2(b), because the update process in OMP removes the influence of $g_{\lambda'_1}$ from $|\langle res_0, g'_k \rangle|$. Accordingly, the maximum value obtained by the second iteration is the second largest value of $|\langle res_0, g'_k \rangle|$, i.e., the value corresponding to n_l . Since the LFM signal has approximate rectangular spectrum in DTSFrFD, so when $k > n_h$, $F_\alpha(m)$ is approximately zero, which leads to an almost constant value of $|\langle res_0, g'_k \rangle|$, as shown in Fig. 2(a). Therefore, after two iterations, the index $\min(\lambda'_1, \lambda'_2)$ corresponds to n_l , which is the initial frequency.

Similarly, Fig. 3 illustrates the relationship between $|\langle res_{i-1}, g_k \rangle|$, $i = 1, 2$ and the fractional “frequency”. And after two iterations, the index $\max(\lambda_1, \lambda_2)$ is corresponding to n_h which is the final frequency.

Thus, the estimated initial frequency is

$$f_0 = u_0 \cdot \csc \alpha = [\min(\lambda'_1, \lambda'_2) \Delta] \cdot \csc \alpha \quad (20)$$

the final frequency estimated is

$$f_1 = u_1 \cdot \csc \alpha = [\max(\lambda_1, \lambda_2) \Delta] \cdot \csc \alpha \quad (21)$$

3.5 Influence of the Fractional Order

According to the analysis above, algorithm 1 can effectively

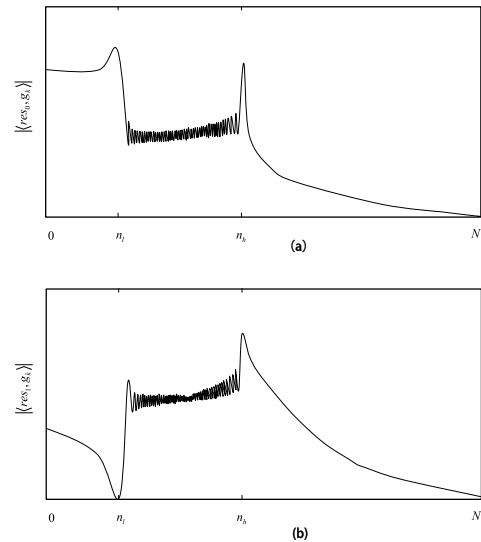


Fig. 3 The relationship between $|\langle res_{i-1}, g_k \rangle|$, and the fractional “frequency”.

extract the edge information of the spectrum in DTSFrFD. Since the α -th-order SFrFT can be regarded as the projection on the rotated frequency axis u , so the spectrum distribution of the signal directly depends on the order of the SFrFT. According to the analysis in Appendix, for a discrete-time LFM signal with the duration of $[-\frac{T_d}{2}, \frac{T_d}{2}]$, its amplitude spectrum in DTSFrFD is

$$|X_\alpha(u)| \approx \frac{A}{\sqrt{K_{lfm} + \cot \alpha}} \cdot \text{rect}\left(\frac{u - 2\pi u_0 \csc \alpha}{B'}\right),$$

when $(K_{lfm} + \cot \alpha / 2\pi) T_d^2 \gg 1$. Where B' is the bandwidth of the spectrum, α is the fractional orders.

when T_d and K_{lfm} are constant, the fluctuation of Fresnel integral decreases as $\cot \alpha$ increases. So the shape of $|X_\alpha(u)|$ is closer to rectangle and the edge feature of the spectrum is more distinct as shown in Fig. 4, which improves the efficiency of Algorithm 1.

4. Simulation and Analysis

4.1 Simulation Configurations

To evaluate the performance of the proposed method, a uniformly sampled chirp signal is tested. The original chirp signal in discrete-time domain is denoted by $x(n)$. The noisy signal is $x(n) + w(n)$, where $w(n)$ is the zero-mean Gaussian noise. The SNR is defined by $10 \log(\|x\|^2 / \|w\|)$. $x(n)$ is given by $x(n) = E e^{j\pi K_{lfm} n^2 / f_{NYQ}^2} \cos(2\pi f_1 n / f_{NYQ})$, where E is the amplitude of the signal which could be random or fixed. $K_{lfm} = 0.200 \times 10^9$ Hz/s is the signal modulation rate. The Nyquist sampling rate is $f_{NYQ} = u_{NYQ} \csc \alpha = 2.2$ GHz, where u_{NYQ} is the sampling rate in FrFD. α is the bandlimited order which varies from -0.50×10^{-8} to -0.36×10^{-8} with a step of -0.01×10^{-8} . The signal duration time is $T = 1$ s. So the bandwidth of $x(n)$ is $B = K_{lfm} \cdot T = 10$ MHz,

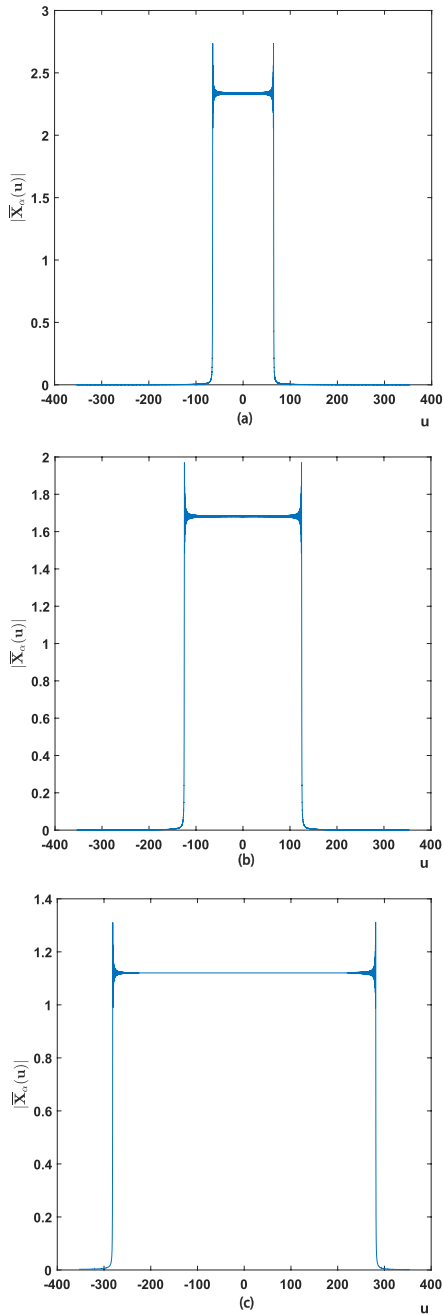


Fig. 4 The amplitude spectrums of the LFM signal in DTSFrFD with different orders ($SNR = 15\text{ dB}$).

$f_l = 1\text{ GHz}$ is the initial frequency. The signal is both frequency bandlimited and fractional bandlimited with different bandwidths in the observation interval. Simulations were conducted to validate parameter estimation accuracy. Each simulation has 300 trials to ensure statistically stable results.

4.2 Parameter Estimation Accuracy

In this experiment, we test the parameter estimation accuracy of our proposed method, compared with the tradi-

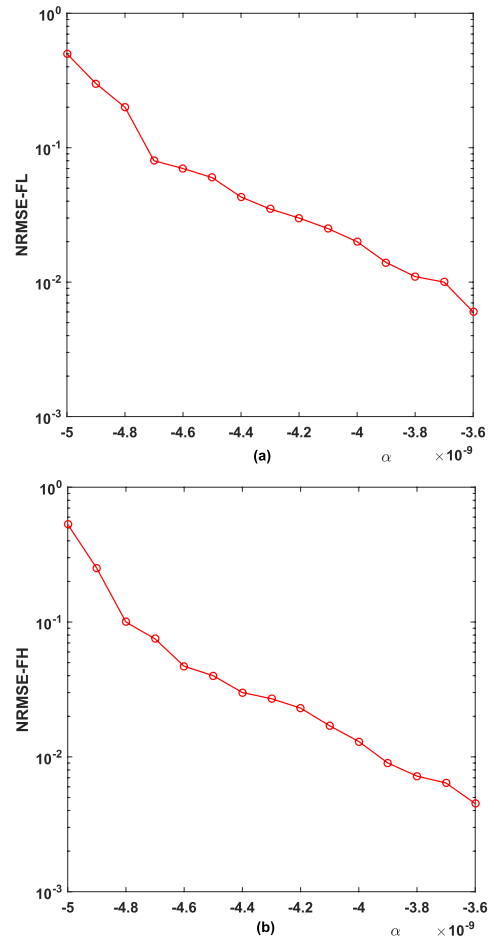


Fig. 5 The performance in the noise-free case.

tional search-based method [11] and reconstruction technique [28]. The parameter estimation accuracy is evaluated by the NRMSE in the noise-free and noisy cases. And the NRMSE is defined as:

$$f_{NRMSE} = \frac{\sqrt{\frac{1}{N} \sum_{n=1}^N (\hat{f}_n - f_n)^2}}{\max(\hat{f}_n) - \min(\hat{f}_n)}$$

Where N is the number of Monte Carlo trials, \hat{f}_n is the estimation signal frequency from the n -th Monte Carlo experiment, f_n is the original signal frequency. Figure 5 depicts the tradeoff between NRMSE and the fractional order α in the noise-free case. The orders α varies from -0.50×10^{-8} to -0.36×10^{-8} with a step of -0.01×10^{-8} . According to the previous analysis, fractional order α may lead to changes in the spectral width. The wider the spectrum, the better estimation performance can be achieved. And it is observed that a smaller NRMSE correspond to larger α and vice versa.

In the noisy case, the simulations demonstrated two aspects: the tradeoff between NRMSE and the fractional order α , and the balance between NRMSE and signal-to-noise ratio (SNR).

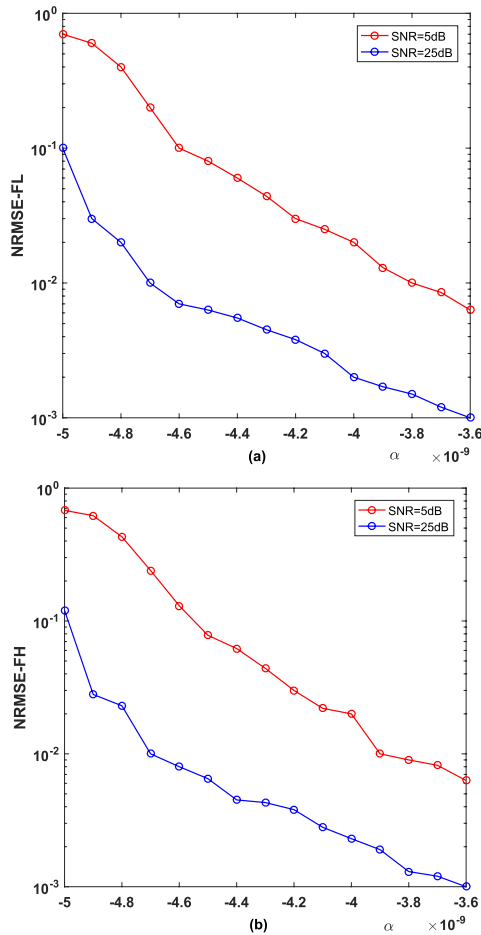


Fig. 6 The relationship between the NRMSE and orders α in the noise case.

Figure 6 shows the relationship between the NRMSE and orders α . In Fig. 6, the SNR is {5, 25} dB, the orders α varies from -0.50×10^{-8} to -0.36×10^{-8} with a step of -0.01×10^{-8} . The increase of α leads to the wider bandwidth and the NRMSE decreases.

In Fig. 7, the SNR varies from -10 dB to 18 dB with a step of 2 dB. The fractional order α is $\{-0.50 \times 10^{-8}, -0.40 \times 10^{-8}\}$. It is common that the NRMSE decreases with increasing SNR in both the proposed method and compared methods. And it is clear that the proposed method has better accuracy.

Figure 8 depicts the performance in terms of NRMSE with different SNRs and fractional order α for the proposed method. The SNR varies from -105 dB to 18 dB with a step of 2 dB. The fractional order α varies from $\{-0.50 \times 10^{-8}\}$ to $\{-0.36 \times 10^{-8}\}$ with a step of $\{-0.02 \times 10^{-8}\}$. It is observed that the NRMSE has the opposite trend as the SNR.

5. Conclusion

This paper introduces a parameter estimation method to determine the initial frequency and final frequency of the fractional bandlimited LFM signals by using OMP. The edge

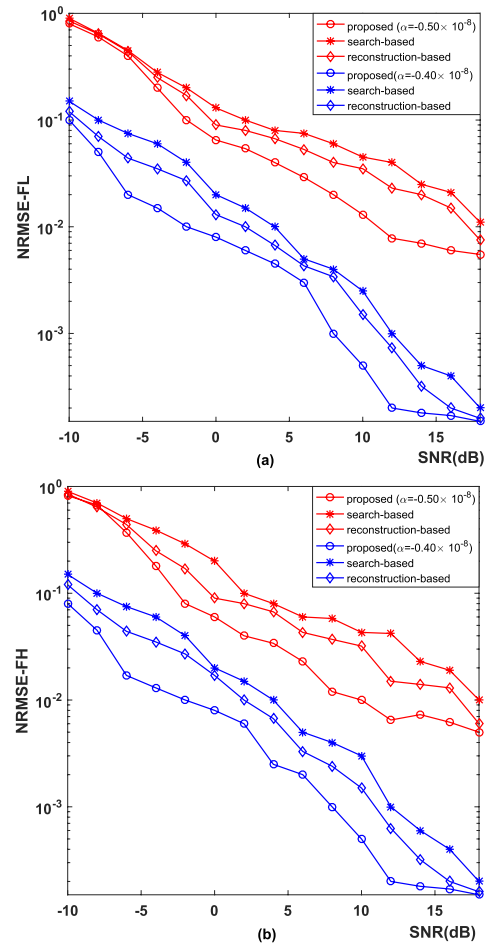


Fig. 7 The relationship between the NRMSE and SNR.

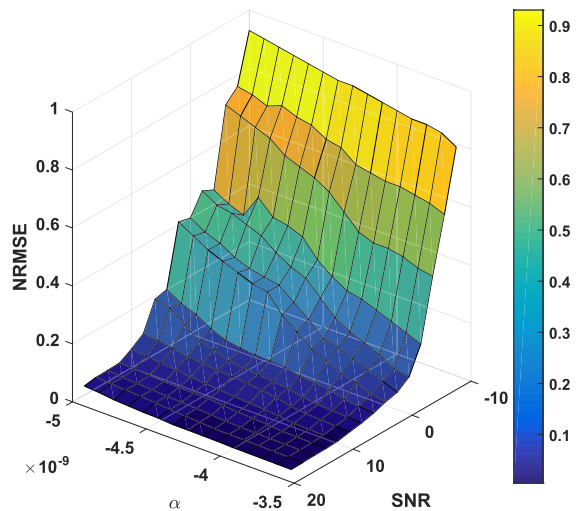


Fig. 8 The relationship between the NRMSE and SNR.

information of the spectrum can be extracted effectively in DTSFrFD, and the corresponding frequencies are obtained. The proposed method avoids reconstruction and the traditional peak-searching procedure, and it only needs two iterations. The theoretical analysis and the simulations results

demonstrate better performance of the proposed method in comparison with existing methods.

Acknowledgments

This work is supported by National Natural Science Foundation of China (No. 61271354) and Henan Province Science and Technology Key Project (No. 142102210431).

References

- [1] A. Serbes, "On the estimation of LFM signal parameters: Analytical formulation," *IEEE Trans. Aerosp. Electron. Syst.*, vol.54, no.2, pp.848–860, 2018.
- [2] H.M. Ozaktas, Z. Zalevsky, and M.A. Kutay, *The Fractional Fourier Transform: With Applications in Optics and Signal Processing*, Wiley, 2001.
- [3] R. Tao, B. Deng, and Y. Wang, "Research progress of the fractional Fourier transform in signal processing," *Sci. China*, vol.49, no.1, pp.1–25, 2006.
- [4] L. Qi, R. Tao, S. Zhou, and Y. Wang, "Detection and parameter estimation of multicomponent LFM signal based on the fractional Fourier transform," *Sci. China Ser. F: Inf. Sci.*, vol.47, no.2, pp.184–198, 2004.
- [5] C. Capus and K. Brown, "Fractional Fourier transform of the Gaussian and fractional domain signal support," *IEE Proceedings - Vision, Image and Signal Processing*, vol.150, no.2, pp.99–106, 2003.
- [6] Y. Zhao, Y. Hua, W. Gang, J.I. Fei, and F. Chen, "Parameter estimation of wideband underwater acoustic multipath channels based on fractional fourier transform," *IEEE Trans. Signal Process.*, vol.64, no.20, pp.5396–5408, 2016.
- [7] X. Liu and C. Wang, "A novel parameter estimation of chirp signal in α -stable noise," *IEICE Electron. Express*, vol.14, no.8, pp.1–11, 2017.
- [8] Y. Liu, Y. Zhao, J. Zhu, Y. Xiong, and B. Tang, "Iterative high-accuracy parameter estimation of uncooperative OFDM-LFM radar signals based on FrFT and fractional autocorrelation interpolation," *Sensors*, vol.18, no.10, pp.3550–3559, 2018.
- [9] L. Tao, Z. Qian, X. Fan, and P. Chen, "Parameter estimation of LFM signal intercepted by improved dual-channel Nyquist folding receiver," *Electron. Lett.*, vol.54, no.10, pp.659–661, 2018.
- [10] J. Song, Y. Liu, and Y. Wang, "Iterative interpolation for parameter estimation of LFM signal based on fractional Fourier transform," *Circuits Syst. Signal Process.*, vol.32, no.3, pp.1489–1499, 2013.
- [11] Y. Chen, L. Guo, and Z. Gong, "The concise fractional Fourier transform and its application in detection and parameter estimation of the linear frequency-modulated signal," *Chinese J. Acoust.*, no.1, pp.70–86, 2017.
- [12] Y.X. Zhang, R.J. Hong, C.F. Yang, Y.J. Zhang, Z.M. Deng, and S. Jin, "A fast motion parameters estimation method based on cross-correlation of adjacent echoes for wideband LFM radars," *Applied Sciences*, vol.7, no.5, p.500, 2017.
- [13] Y. Jin and D. GAO, "Parameter estimation of LFM signals based on synchrosqueezing chirplet transform in complicated noise," *J. Electron. Inf. Technol.*, vol.39, no.8, pp.1906–1912, 2017.
- [14] S. Barbarossa, "Analysis of multicomponent LFM signals by a combined Wigner-Hough transform," *IEEE Trans. Signal Process.*, vol.43, no.6, pp.1511–1515, 1995.
- [15] G. Bai, Y. Cheng, W. Tang, and S. Li, "Chirp rate estimation for LFM signal by multiple DPT and weighted combination," *IEEE Signal Process. Lett.*, vol.26, no.1, pp.149–153, 2019.
- [16] F.G. Geroleo and M. Brandt-Pearce, "Detection and estimation of LFM radar signals," *IEEE Trans. Aerosp. Electron. Syst.*, vol.48, no.1, pp.405–418, 2012.
- [17] T. Jensen, J.K. Nielsen, J.R. Jensen, M.G. Christensen, and S.H. Jensen, "A fast algorithm for maximum likelihood estimation of harmonic chirp parameters," *IEEE Trans. Signal Process.*, vol.65, no.19, pp.5137–5152, 2017.
- [18] D. Fourier, F. Auger, K. Czarnecki, S. Meignen, and P. Flandrin, "Chirp rate and instantaneous frequency estimation: Application to recursive vertical synchrosqueezing," *IEEE Signal Process. Lett.*, vol.24, no.11, pp.1724–1728, 2017.
- [19] X. Meng, A. Jakobsson, X. Li, and Y. Lei, "Estimation of chirp signals with time-varying amplitudes," *Signal Process.*, vol.147, pp.1–10, 2018.
- [20] Y. Doweck, A. Amar, and I. Cohen, "Fundamental initial frequency and frequency rate estimation of random amplitude harmonic chirps," *IEEE Trans. Signal Process.*, vol.63, no.23, pp.6213–6228, 2015.
- [21] W. Yi, Z. Chen, R. Hoseinnezhad, and R.S. Blum, "Joint estimation of location and signal parameters for an LFM emitter," *Signal Process.*, vol.134, pp.100–112, 2017.
- [22] D. Ding, N. Cheng, and Y. Liao, "LFM signal parameters estimation using optimization approach initialized by Lipschitz constant assisted DIRECT algorithm," *Circuits, Syst. Signal Process.*, vol.34, no.6, pp.2037–2051, 2015.
- [23] L. Applebaum, S.D. Howard, S. Searle, and R. Calderbank, "Chirp sensing codes: Deterministic compressed sensing measurements for fast recovery," *Appl. Comput. Harmon. Anal.*, vol.26, no.2, pp.283–290, 2009.
- [24] S.I. Adalbjörnsson, A. Jakobsson, and M.G. Christensen, "Multi-pitch estimation exploiting block sparsity," *Signal. Process.*, vol.109, pp.236–247, 2015.
- [25] L. Gao, S.-Y. Su, and Z.-P. Chen, "Orthogonal sparse representation for chirp echoes in broadband radar and its application to compressed sensing," *J. Electron. Inform. Technol.*, vol.33, no.11, pp.2720–2726, 2011.
- [26] B. Fang, G.M. Huang, and J. Gao, "A multichannel blind compressed sensing framework for linear frequency modulated wideband radar signals," *Zidonghua Xuebao/acta Automatica Sinica*, vol.41, no.3, pp.591–600, 2015.
- [27] L. Hu, J. Xiong, Z.Z. Guang, and S.Q. Fu, "Compressed sensing of superimposed chirps with adaptive dictionary refinement," *Sci. China Inf. Sci.*, vol.56, no.12, pp.1–15, 2013.
- [28] B. Fang, G. Huang, J. Gao, and W. Zuo, "Compressive sensing of linear frequency modulated echo signals in fractional Fourier domains," *J. Xidian University*, vol.42, no.1, pp.200–206, 2015.
- [29] L.B. Almeida, "The fractional fourier transform and time-frequency representations," *IEEE Trans. Signal Process.*, vol.42, pp.3084–3091, 1994.
- [30] S.C. Pei and J.J. Ding, "Simplified fractional fourier transforms," *J. Opt. Soc. Am. A*, vol.17, no.12, pp.2355–2367, 2000.

Appendix:

Spectrum distribution characteristics of LFM signal in SFrFD

A monocomponent LFM signal is defined by:

$$x(t) = A \cdot \exp x(j2\pi f_0 t + j\pi K_{lfm} t^2) \quad (\text{A} \cdot 1)$$

Where f_0 is the initial frequency. A is the amplitude of $x(t)$ which could be random or fixed. K_{lfm} is the modulation rate.

And the duration time of $x(t)$ is $\left[-\frac{T_d}{2}, \frac{T_d}{2}\right]$.

The SFrFT of $x(t)$ can be calculated by

$$\bar{X}_\alpha(u) = A (j2\pi)^{-1/2} \int_{-\infty}^{\infty} \exp(-jut + jt^2 \cot \alpha/2) \cdot \exp(j2\pi f_0 t + j\pi K_{lfm} t^2) dt$$

$$= A (j2\pi)^{-1/2} \int_{-\infty}^{\infty} \exp(j\pi(K'_{l_{fm}} + \cot \alpha/2\pi)t^2 + j2\pi f_0 t) \cdot \exp(-jut) dt \quad (\text{A} \cdot 2)$$

According to (A.2), $\bar{X}_\alpha(u)$, the SFrFT of $x(u)$, denotes the FT of another LFM signal whose modulation rate is $K'_{l_{fm}} = K_{l_{fm}} + \cot \alpha/2\pi$, initial frequency is f_0 , and the frequency interval is $[f_0 - K'_{l_{fm}} \frac{T_d}{2}, f_0 + K'_{l_{fm}} \frac{T_d}{2}]$. So the bandwidth is $B' = K'_{l_{fm}} \cdot T_d$. It can be interpreted that the SFrFT rotates the time-frequency distribution curve of $x(t)$ in the clockwise direction with angle α , so that the modulation rate and bandwidth changes.

Thus,

$$\bar{X}_\alpha(u) = \frac{A}{\sqrt{2K'_{l_{fm}}}} \exp\left(-\frac{j(u-2\pi u_0 \csc \alpha)^2}{4\pi K'_{l_{fm}}}\right) \cdot \{[c(u_2) + c(u_1)] + j[s(u_2) + s(u_1)]\}$$

Where

$$c(u) = \int_0^u \cos\left(\frac{\pi}{2}x^2\right) dx$$

and

$$s(u) = \int_0^u \sin\left(\frac{\pi}{2}x^2\right) dx$$

is the Fresnel integral. And

$$\begin{cases} u_1 = \sqrt{2K'_{l_{fm}}}\left(\frac{T_d}{2} - \frac{u-2\pi u_0 \csc \alpha}{K'_{l_{fm}}}\right) \\ u_2 = \sqrt{2K'_{l_{fm}}}\left(\frac{T_d}{2} + \frac{u-2\pi u_0 \csc \alpha}{K'_{l_{fm}}}\right) \end{cases} \quad (\text{A} \cdot 3)$$

where $u_0 = f_0 \sin \alpha$.

So the amplitude spectrum of $\bar{X}_\alpha(u)$ is

$$|X_\alpha(u)| = \frac{A}{\sqrt{2K'_{l_{fm}}}} \cdot \{[c(u_2) + c(u_1)]^2 + [s(u_2) + s(u_1)]^2\}^{1/2} \quad (\text{A} \cdot 4)$$

and the phase spectrum is

$$\begin{aligned} \theta(u) &= \theta_1(u) + \theta_2(u) \\ &= -\frac{(u-2\pi u_0 \csc \alpha)^2}{4\pi K'_{l_{fm}}} + \arctan\left[\frac{s(u_2) + s(u_1)}{c(u_2) + c(u_1)}\right] \end{aligned} \quad (\text{A} \cdot 5)$$

Substituting $K'_{l_{fm}} = \frac{B'}{T}$ into Eq. (A.5):

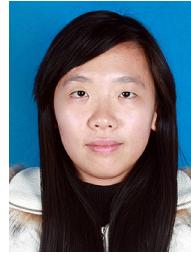
$$\begin{cases} u_1 = \sqrt{2B'T_d}\left(\frac{1}{2} - \frac{u-2\pi u_0 \csc \alpha}{B'}\right) \\ u_2 = \sqrt{2B'T_d}\left(\frac{1}{2} + \frac{u-2\pi u_0 \csc \alpha}{B'}\right) \end{cases} \quad (\text{A} \cdot 6)$$

According to the property associated with Fresnel integral, when $B'T_d \gg 1$, i.e. $K'_{l_{fm}}T_d^2 \gg 1$, $c(u_2) \approx s(u_2) \approx \frac{1}{2}$, so

$$|X_\alpha(u)| \approx \frac{A}{\sqrt{K'_{l_{fm}}}} \cdot \text{rect}\left(\frac{u-2\pi u_0 \csc \alpha}{B'}\right)$$

$$\begin{aligned} &= \frac{A}{\sqrt{K'_{l_{fm}} + \cot \alpha/2\pi}} \cdot \text{rect}\left(\frac{u-2\pi u_0 \csc \alpha}{B'}\right), \\ \theta(u) &\approx -\frac{\pi(u-2\pi u_0 \csc \alpha)^2}{K'_{l_{fm}}} + \frac{\pi}{4} \\ &= -\frac{\pi(u-2\pi u_0 \csc \alpha)^2}{K'_{l_{fm}} + \cot \alpha/2\pi} + \frac{\pi}{4}. \end{aligned}$$

Therefore, when $(K'_{l_{fm}} + \cot \alpha/2\pi)T_d^2 \gg 1$, $|X_\alpha(u)|$ is approximately a rectangular spectrum.



Xiaomin Li received the B.Eng. degree in electronic engineering from Nanjing University of Science and Technology, China, in 2011. Currently she is a research student working towards the Ph.D. degree in Nanjing University of Science and Technology, China. Her research interests include information processing and time-frequency analysis for communication signals.



Huali Wang received the Ph.D. degree in electronic engineering from the Nanjing University of Science and Technology, China, in 1997. He is currently a Professor with the College of Communication Engineering, The Army Engineering University of PLA, Nanjing, China. His research interests include satellite communication and signal processing.



Zhangkai Luo received the B.Eng. degree in measurement, control and instruments from Hebei University of Technology, Tianjin, China, in 2011. Currently he is a research student working towards the Ph.D. degree in PLA University of Science and Technology, China. His research interests include information processing and confrontation.